ADVANCED FUNCTIONAL MATERIALS
www.afm-journal.de

Materials Views
www.MaterialsViews.com

Influence of Substituted Pyridine Rings on Physical Properties and Electron Mobilities of 2-Methylpyrimidine Skeleton-Based Electron Transporters

Hisahiro Sasabe, Daisaku Tanaka, Daisuke Yokoyama, Takayuki Chiba, Yong-Jin Pu, Ken-ichi Nakayama, Masaaki Yokoyama, and Junji Kido**

A series of 2-methylpyrimidine skeleton-based electron-transporting derivatives (BPyMPM) are designed and synthesized to investigate the influence of substituted pyridine rings on the physical properties and electron mobilities (μ_e). The only structural difference is the position of substituted pyridine rings. The melting point (*T*m) of B4PyMPM is estimated to be ca. 50 °C higher than that of B3PyMPM, and ca. 120 °C higher than that of B2PyMPM. The ionization potential is observed to increase in the order B2PyMPM (6.62 eV) < B3PyMPM (6.97 eV) < B4PyMPM (7.30 eV), measured using ultraviolet photoelectron spectroscopy. Furthermore, time-of-fight measurements of vacuum-deposited films demonstrate that the μ_e at 298 K of B4PyMPM is 10 times higher than that of B3PyMPM and 100 times higher than that of B2PyMPM. To extract the charge transport parameters, the temperature and field dependencies of μ_e are investigated. Using Bässler's disorder formalism, the degree of energetic disorder is estimated to decrease in the order B2PyMPM (91 meV) > B3PyMPM (88 meV) > B4PyMPM (76 meV), and the positional disorder is 2.7 for B2PyMPM, and < 1.5 for B3PyMPM and B4PyMPM.

1. Introduction

Organic light-emitting devices (OLEDs) are expected to be applied as eco-friendly solid-state lighting and next-generation flat-display panels.[1] To improve the efficacy of OLEDs, a reduction in the electrical power consumption is absolutely essential. Phosphorescent emitters such as $Ir(ppy)_3$ and FIrpic increase the efficacy to as high as 100%, allowing the realization of high-efficiency OLEDs.[2,3] By using these phosphorescent emitters, our group has developed high-efficiency sky-blue,[4] green[5] and white[6] OLEDs with external quantum efficiencies of up to 29% without any out-coupling enhancement. These remarkable advances have been achieved by developing novel phosphorescent materials. In particular, multifunctional electron-transporting materials (ETMs) can simplify the structure of multilayer devices, leading to a reduction in cost. Therefore, the development of ETMs with functionalities such as (i) high electron injection, (ii) high electron mobility (μ_e), (iii) high hole-blocking ability and (iv) high triplet energy (E_{T1}), to suppress exciton quenching, is critical.[7] However, there are very few papers providing an effective molecular design for such an ETM. Recently, Su and co-workers reported the structure–property relationships of 1,3,5-tri(*m*-pyridylphenyl)benzene (TmPyPB) derivatives and revealed that the position of substituted pyridine rings was a key factor in determining the electron-injection properties and OLED performances.[8] To get more insight into the origin of electron-transporting properties, a fundamental understanding of the structural parameters is necessary.

Here, we demonstrate the influence of the position of substituted pyridine rings on the fundamental physical properties and the μ_e of bis-4,6-(3,5-dipyridylphenyl)-2-methylpyrimidine (BPyMPM) derivatives.[5a] In addition, to extract the charge-transport parameters, the temperature and field dependencies of μ_e were investigated using the time-of-flight (TOF) method. Using Bässler's disorder formalism,[9] the degrees of energetic disorder (σ) and positional disorder (Σ) were also estimated. Finally, the origin of these charge-transport parameters is discussed.

2. Results and Discussion

2.1. DFT Calculations

To estimate the effect of the 2-methylpyrimidine skeleton, we conducted density functional theory (DFT) calculations for four molecules: B2PyMPM, B3PyMPM, B4PyMPM, and

Dr. H. Sasabe, Prof. J. Kido
Department of Organic Device Engineering
Yamagata University
4–3-16 Jonan, Yonezawa, Yamagata 992–8510, Japan
E-mail: h-sasabe@yz.yamagata-u.ac.jp; kid@yz.yamagata-u.ac.jp
Dr. D. Tanaka, Dr. D. Yokoyama, T. Chiba, Dr. Y.-J. Pu,
Dr. K. Nakayama, Prof. M. Yokoyama
Department of Organic Device Engineering
Yamagata University
4–3-16 Jonan, Yonezawa, Yamagata 992–8510, Japan

DOI: 10.1002/adfm.201001252

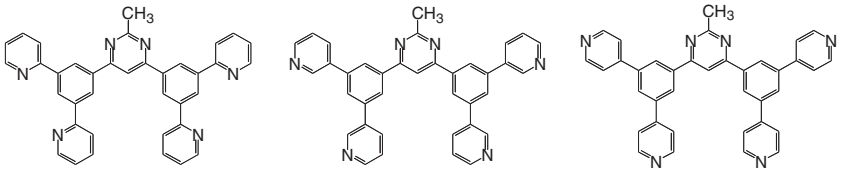

Figure 1. Chemical structure of BPyMPM derivatives.

2,9-dimethyl-4,7-diphenylphenanthroline (BCP) as a reference (**Figure 1**). Here, the only structural difference between the BPyMPM derivatives is the position of substituted pyridine rings (2-pyridine for B2PyMPM, 3-pyridine for B3PyMPM, and 4-pyridine for B4PyMPM, respectively). The optimized structures were calculated at the RB3LYP 6–31G(d) level for the ground state, and at UB3LYP 6–31G(d) for the excited triplet state. The single-point energies were calculated at the corresponding 6–311+G(d,p) levels. The vertical ionization energies (I_p) and electron affinities (E_a) were obtained using the ΔSCF method. Here, the single-point energies of radical ion species were calculated at the UB3LYP 6–311+G(d,p) level using the optimized ground-state structures. In addition, using the previously reported method,[10] the E_{T1} energies of BPyMPM derivatives were calculated. All the calculated values are summarized in **Table 1**.

The I_p was shown to increase in the order B2PyMPM (7.36 eV) < BCP (7.40 eV) < B3PyMPM (7.81 eV) < B4PyMPM (8.17 eV). Similarly, the E_a increased in the order BCP (0.47 eV) < B2PyMPM (0.90 eV) < B3PyMPM (1.30 eV) < B4PyMPM (1.47 eV). The BPyMPM derivatives have deep I_ps similar to that of BCP but much lower-lying E_as than that of BCP. Thus, these compounds are expected to have both high hole-blocking and favorable electron-injection properties. All the E_{T1}s of the BPyMPM derivatives were estimated to be ca. 0.4 eV higher than those of BCP, suggesting their practical use for blue and green phosphorescent OLEDs.

2.2. Synthesis

The synthetic route to BPyMPM derivatives is shown in **Scheme 1**. All the BPyMPM derivatives can be easily prepared on a multigram scale within 3 steps. The precursor **3** was prepared via the Suzuki–Miyaura coupling reaction of 4,6-dichloro-2-methylpyrimidine (**1**) with 3,5-dichlorophenyboronic acids (**2**) with an 81% yield using a $PdCl_2(PPh_3)_2$/Na_2CO_3/CH_3CN catalyst system.[11] The resulting tetrachloride (**3**) was coupled with an excess of 3-pyridine boronate ester (**4**) or 4-pyridine boronate ester (**5**) to afford B3PyMPM in 77% yield and B4PyMPM in 67% yield, respectively.[12] On the other hand, the 2-pyridine derivative, B2PyMPM, was prepared via the Miyaura–Ishiyama borylation of **3** with bis(pinacolato)diboron (**6**). The tetraboronate ester (**7**) was obtained in 61% yield.[13] The Suzuki–Miyaura coupling reaction of **7** with 2-bromopyridine (**8**) afforded B2PyMPM in 84% yield.[14] The characterization of compounds was established on the basis of mass spectrometry, NMR, and elemental analyses, and the compounds were purified by train sublimation before device fabrication.

Table 1. Calculated I_p, E_a and E_{T1} values of BPyMPM derivatives.

Compound	I_p [eV][a]	E_g [eV][b]	E_a [eV][c]	E_{T1} [eV][d]
B2PyMPM	7.36	6.46	0.90	3.04
B3PyMPM	7.81	6.51	1.30	3.08
B4PyMPM	8.17	6.70	1.47	3.07
BCP	7.40	6.93	0.47	2.62

[a]Ionization potential. [b]Energy gap ($E_g = I_p - E_a$). [c]Electron affinity. [d]Triplet energy.

2.3. TLC and Solubility Analyses

Thin layer chromatography (TLC, silica gel) analysis using chloroform/methanol (30:1 v/v) as an eluent showed that the retention factors (R_f) decreased in the order B2PyMPM (0.80) >> B3PyMPM (0.25) > B4PyMPM (0.12). Therefore, the degree of the interaction with silica gel, which shows the strength of the hydrogen-bonding interactions between a single substrate molecule and silanol, is found to increase in the order B2PyMPM << B3PyMPM < B4PyMPM. Next, we checked the solubility of BPyMPM derivatives, and found that BPyMPM derivatives were hardly soluble in ordinary solvents except halogenated solvents, such as chloroform and dichloromethane. Among BPyMPM derivatives, B3PyMPM and B4PyMPM were found to be much less soluble in chloroform compared with B2PyMPM. On the other hand, all the BPyMPM derivatives were highly soluble in chloroform/methanol mixtures (for example, 30:1 v/v). Since the H-bonding interactions are cleaved by methanol, these observations strongly suggest the presence of the intermolecular CH–N hydrogen-bonding interactions in the solid state and that the degree of the interactions increased in the order B2PyMPM << B3PyMPM < B4PyMPM.

2.4. Physical Properties

All the physical properties are summarized in **Table 2**. The thermal properties of the BPyMPM derivatives were estimated by differential scanning calorimetry (DSC) and thermogravimetric analysis (TGA). The glass transition temperature (T_g) of B2PyMPM was observed at 107 °C, indicating thermal stability of the thin film. On the other hand, T_g was not detected in the cases of B3PyMPM and B4PyMPM. A weight loss of only 5% (T_{d5}) for the BPyMPM derivatives was found at over 465 °C, indicating a high thermal stability. The melting point (T_m) of B4PyMPM was observed to be ca. 50 °C higher than that of B3PyMPM, and ca. 120 °C higher than that of B2PyMPM. Because the only difference between derivatives is the position of the substituted pyridine rings, these results may be mainly due to the above-mentioned H-bonding interactions

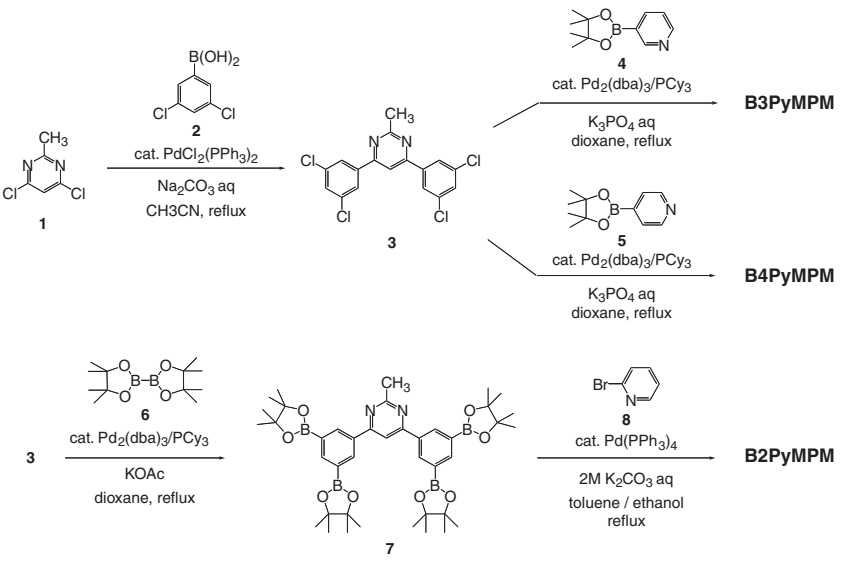

Scheme 1. Synthesis of BPyMPM derivatives.

in the solid state. Thus, the degree of these interactions is considered to increase in the order B2PyMPM < B3PyMPM < B4PyMPM. This consideration is consistent with the TLC analysis.

The optical properties were determined by ultraviolet photoelectron spectroscopy (UPS) and UV–vis absorption spectroscopy. The $I_p$was observed at 6.62 eV for B2PyMPM, 6.97 eV for B3PyMPM and 7.30 eV for B4PyMPM. The E_a was estimated by subtraction of the optical energy gap (E_g) from the I_p to be 3.07 eV for B2PyMPM, 3.44 eV for B3PyMPM and 3.71 eV for B4PyMPM (Table 2). As predicted from the DFT calculations, BPyMPM derivatives have deep I_ps to block holes as well as low-lying E_as for electron injection, and both the I_p and E_a were observed to increase in the order B2PyMPM < B3PyMPM < B4PyMPM. Although the structural difference is very small, the differences in the I_p and E_a values are quite large. The position of substituted pyridine rings is the key factor for determining the optical properties.

In general, the n–π^* transition is known as the forbidden transition and its absorption band is very weak. However, in the UV–vis absorption spectra from 290 to 330 nm, a strong n–π^* absorption was observed for the solid films, and the degree of the n–π^* absorption decreased in the order B2PyMPM > B3PyMPM > B4PyMPM (see Supporting Information). Next, we attempted to measure the photoluminescent spectra both of the films and of solutions in chloroform. However, emission was not detectable from all the films by using the excitation light of λ_{ex} = 250 nm. On the other hand, in chloroform solutions, very weak emission with a peak wavelength around 400 nm was detectable (see Supporting Information). According to the El-Sayed rule,[15] the mixing between the ^{1}n–π^* state and the $^3\pi$–π^* state is very large, and intersystem crossing can easily occur from the ^{1}n–π^* state. Thus, in the case of BPyMPM derivatives, non-radiative decay from the $^3\pi$–π^* state is considered to mainly occur via intersystem crossing from the ^{1}n–π^* state. In fact, relatively-strong phosphorescence was observed from all the films at 4.2 K. The E_{T1} levels were determined from the onset of the phosphorescent spectra, and were estimated to be 2.75 eV for B2PyMPM, 2.75 eV for B3PyMPM, and 2.80 eV for B4PyMPM (see Supporting Information). As predicted from the DFT calculations, BPyMPM derivatives are applicable for green and blue phosphorescent OLEDs.

2.5. Electron Mobilities

To evaluate the electron mobility, we carried out TOF measurements of the BPyMPM derivatives. The device structure was [ITO (110 nm)/BPyMPM derivatives/Al (100 nm)], and the sample thickness was 8.0 μm for B2PyMPM, 7.5 μm for B3PyMPM, and 7.2 μm for B4PyMPM. **Figure 2** shows representative transient TOF of electrons measured at room temperature. All the transient photocurrent signals were dispersive, suggesting the presence of electron traps. The μ_es were on the order of 10^{-6} $cm^2V^{-1}s^{-1}$ for B2PyMPM, 10^{-5} cm^2 V^{-1} s^{-1} for B3PyMPM and 10^{-4} cm^2 V^{-1} s^{-1} for B4PyMPM at 6.4×10^{-5} V cm^{-1}. Compared with conventional ETMs such as Alq_3 and 3-(4-biphenylyl)-4-phenyl-5-(4-*tert*-butylphenyl)-1,2,4-triazole, the μ_e of B4PyMPM was estimated to be 100 times higher.[5] Because the μ_e of B4PyMPM was estimated to be 10 times higher than that of B3PyMPM and 100 times higher than that of B2PyMPM, it is clear that the nitrogen position in the pyridine rings strongly affects the μ_e. This tendency is very similar to that of 2-phenyl-4,6-bis(3,5-dipyridylphenyl)pyrimidine

Table 2. Physical properties of BPyMPM derivatives.

Compound	I_p[eV][a]	E_g [eV][b]	E_a [eV][c]	T_g [°C][d]	T_m [°C][d]	T_{d5} [°C][e]	E_{T1} [eV][f]	μ_e [cm^2 V^{-1} s^{-1}][g]
B2PyMPM	6.62	3.55	3.07	107	257	465	2.75	1.6×10^{-6}
B3PyMPM	6.97	3.53	3.44	n.d.	326	484	2.75	1.5×10^{-5}
B4PyMPM	7.30	3.59	3.71	n.d.	374	472	2.80	1.0×10^{-4}

[a]Ionization potential obtained from UPS. [b]Taken as the point of intersection of the normalized absorption spectra. [c]Calculated using I_p and E_g. [d]Determined by DSC measurement. [e]Obtained from TGA analysis. [f]Onset of phosphorescence measured by using a streak camera (C4334 from Hamamatsu Photonics). [g]Determined by TOF measurement.

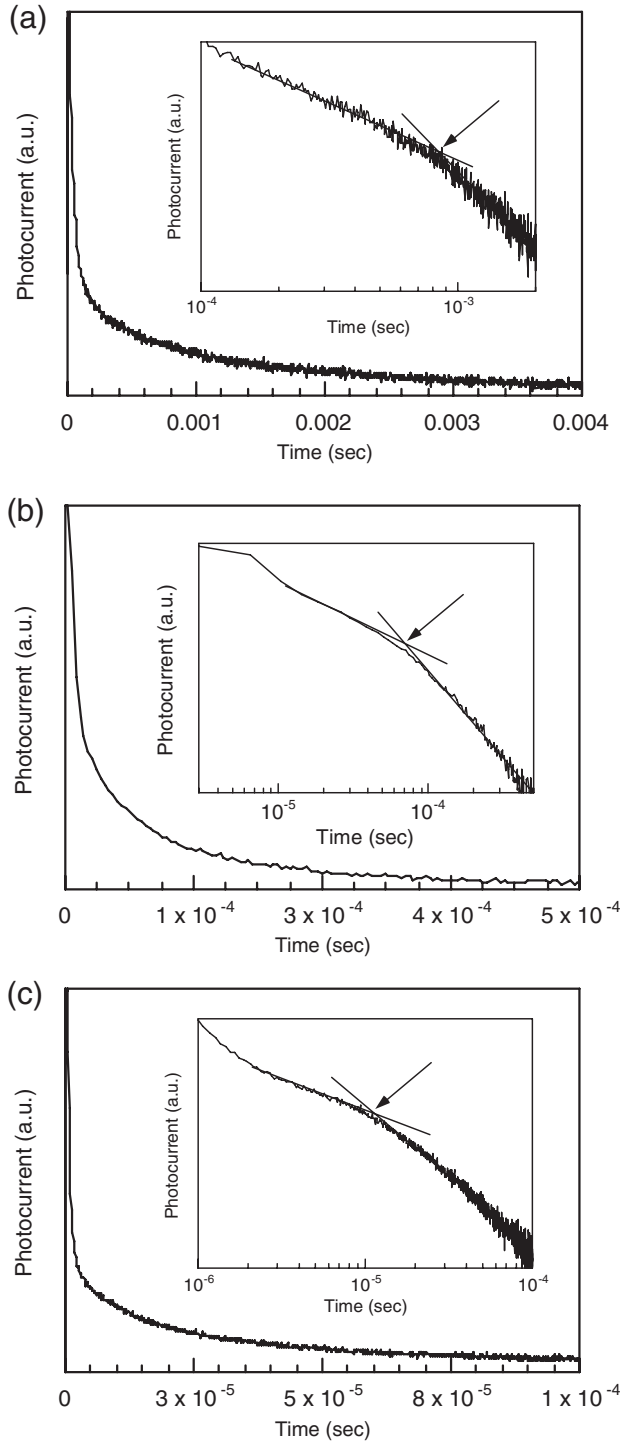

Figure 2. Representative TOF transients for electrons at room temperature: a) B2PyMPM at an electric field ($E^{1/2}$) = 775 (V cm^{-1})$^{1/2}$, b) B3PyMPM at $E^{1/2}$ = 800 (V cm^{-1})$^{1/2}$, c) B4PyMPM at $E^{1/2}$ = 800 (V cm^{-1})$^{1/2}$. Sample thickness was 8.0 μm for B2PyMPM, 7.5 μm for B3PyMPM and 7.2 μm for B4PyMPM, respectively. Insets: Double logarithmic plot.

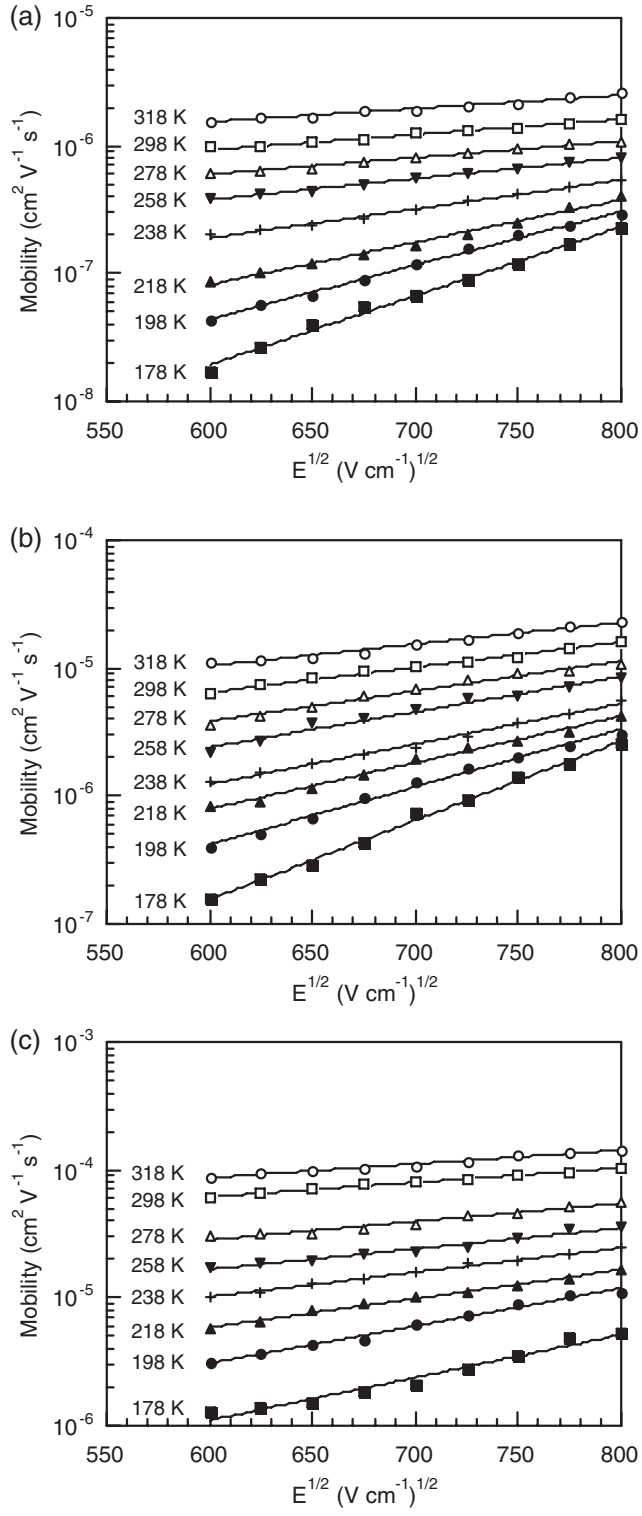

Figure 3. The temperature dependence of field-dependent mobility: a) B2PyMPM, b) B3PyMPM, c) B4PyMPM.

derivatives. On the other hand, it is clearly different from that of TmPyPB derivatives, which have μ_e values almost on the same order without any influence from the position of substituted pyridine rings.[8a] Therefore, to get more insight into the origin of such electron-transporting properties, a fundamental understanding of the structural parameters is necessary.

2.6. Temperature and Field Dependence of Electron Mobilities

In this section, we investigate the temperature and field dependencies of the μ_e and discuss the origin of these charge-transport parameters using Bässler's disorder formalism.[9]

To extract these parameters, the temperature and field dependencies were investigated using the TOF method, and the results are shown in **Figure 3**. Applying Bässler's disorder formalism, the energetic disorder (σ) and positional disorder (Σ) were also estimated. According to Monté Carlo simulations, the temperature and field dependencies of μ are given as, where $\Sigma \geq 1.5$:

$$\mu = \mu_0 \exp\left[-\left(\frac{2\sigma}{3k_B T}\right)^2\right] \exp\left\{C\left[\left(\frac{\sigma}{k_B T}\right)^2 - \Sigma^2\right]\sqrt{E}\right\} \quad (1)$$

If $\Sigma < 1.5$, the temperature and field dependencies of μ are given as:

$$\mu = \mu_0 \exp\left[-\left(\frac{2\sigma}{3k_B T}\right)^2\right] \exp\left\{C\left[\left(\frac{\sigma}{k_B T}\right)^2 - 2.25\right]\sqrt{E}\right\} \quad (2)$$

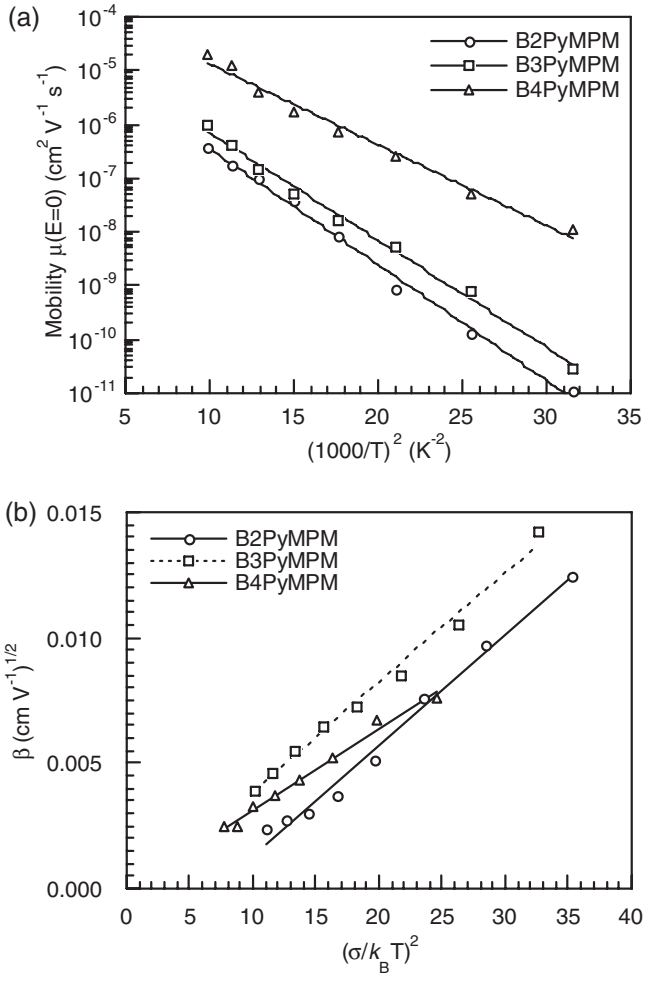

Figure 4. a) Plot of the zero-field mobility $\mu(E = 0)$ vs $(1000/T)^2$. b) Plot of β vs $(\sigma/k_B T)^2$.

Table 3. Electron transport parameters of BPyMPM derivatives.

Compound	μ_0 [cm^2 V^{-1} s^{-1}][a)]	σ [meV][b)]	Σ[c)]	C [(cm V)$^{1/2}$][d)]
B2PyMPM	5.1×10^{-5}	91	2.7	4.4×10^{-4}
B3PyMPM	6.9×10^{-5}	88	1.2	4.4×10^{-4}
B4PyMPM	4.5×10^{-4}	76	0.6	3.3×10^{-4}

[a)]Hypothetical mobility in the disorder-free system. [b)]Energetic disorder. [c)]Positional disorder. [d)]Empirical constant.

where μ_0 is a hypothetical mobility in the disorder-free system, k_B is Boltzmann's constant, E is the electric field, T is the temperature, and C is an empirical constant. The electron-transport parameters μ_0 and σ were obtained by plotting $\log(\mu(E = 0))$ against $(1000/T)^2$(**Figure 4**a). The positional disorder parameter Σ and the values of C were obtained from extrapolation of the slope of the plot of β vs $(\sigma/k_B T)^2$, where $\beta = C[(\sigma/k_B T)^2 - \Sigma^2]$ (**Table 3** and Figure 4b).

The energetic disorder is the fluctuation of hopping-site energy, and shows both intramolecular and intermolecular contributions. In this case, the σ values were on a similar order to that of the standard deviation for the density-of-states (DOS) distribution (≈100 meV),[16] and decreased in the order B2PyMPM (91 meV) > B3PyMPM (88 meV) > B4PyMPM (76 meV). For the intramolecular contribution, the number of conformers decrease in the order B2PyMPM = B3PyMPM > B4PyMPM considering the free rotation of terminal pyridine rings. On the other hand, the intermolecular contribution is attributed to the fluctuation of polarization energy, which is derived from charge-dipole and van der Waals interactions between a charge and the surrounding molecule. Taking this σ order into account, it can be considered that the intermolecular contribution decreases in the order B2PyMPM > B3PyMPM > B4PyMPM. Since this order is the opposite of the degree of the H-bonding interactions, a possible explanation is the influence of molecular orientations. Assuming that the vacuum-deposited BPyMPM molecules can be oriented in the order B2PyMPM < B3PyMPM < B4PyMPM using intermolecular H-bonding interactions, the fluctuation of polarization energy can decrease in the order B2PyMPM > B3PyMPM > B4PyMPM. To confirm this hypothesis, an investigation of molecular orientations is necessary.[17]

The positional disorder describes the fluctuation of the intermolecular distance. In this case, the Σ was evaluated to be 2.7 for B2PyMPM, and $\Sigma < 1.5$ for B3PyMPM and B4PyMPM. Considering that B4PyMPM had a relatively large μ_0, the intermolecular distance is probably shorter and well-ordered molecular orientations can be assumed for the vacuum-deposited B4PyMPM film. Combining the values for all the electron-transport parameters (μ_0, σ, and Σ) and the fact that the intermolecular CH–N hydrogen-bonding interactions can cause self-complementary systems[18] to form graphite-like 2D sheet structures,[19] our results strongly suggest that the vacuum-deposited B4PyMPM film has a well-ordered molecular orientation as well as dense-packing, derived from the H-bonding interactions and leading to a high μ_e.[20] Finally, the difference between the dipole moments may also affect the μ_e, because the dipole moment of B4PyMPM is qualitatively smaller than that of B2PyMPM and B3PyMPM.[21] A further discussion about the dipole moments will be reported soon in a separate paper.

3. Conclusions

A series of 2-methylpyrimidine skeleton-based ETMs, B2PyMPM, B3PyMPM and B4PyMPM, were designed and synthesized. The only structural difference is the position of substituted pyridine rings. DFT calculations predicted that BPyMPM derivatives had different I_p and E_a values depending on the position of the substituted pyridine rings. As predicted from the calculations, the I_ps were observed using UPS to increase in the order B2PyMPM (6.62 eV) < B3PyMPM (6.97 eV) < B4PyMPM (7.30 eV). From both TLC and DSC analyses, the degree of the H-bonding interactions is considered to increase in the order B2PyMPM << B3PyMPM < B4PyMPM. Moreover, TOF measurements of vacuum-deposited films were carried out to determine the μ_e at 298 K: the μ_e of B4PyMPM was on the order of 10^{-4} cm^{-2} V^{-1} s^{-1} at an electric field of 6.4×10^{-5} V cm^{-1}. The μ_e of B4PyMPM was measured to be 10 times higher than that of B3PyMPM and 100 times higher than that of B2PyMPM. Furthermore, the temperature and field dependencies of $\mu_e$were investigated to extract the charge-transport parameters. Using Bässler's disorder formalism, the degree of σ was estimated to decrease in the order B2PyMPM (91 meV) > B3PyMPM (88 meV) > B4PyMPM (76 meV) due to the number of conformers and intermolecular H-bonding interactions. Similarly, the Σ was evaluated to be 2.7 for B2PyMPM, and $\Sigma < 1.5$ for B3PyMPM and B4PyMPM. Considering the relatively high μ_0 of B4PyMPM, the intermolecular distance are shorter and well-ordered molecular orientations are assumed due to the H-bonding interactions occurring in the vacuum-deposited B4PyMPM film. These results clearly indicate that the position of substituted pyridine rings is critically important to adjust the fundamental physical properties and the μ_e. Our findings provide not only a powerful guideline to design ETMs but also a new way to control the molecular aggregation states of vacuum-deposited films using the weak intermolecular CH–N hydrogen-bonding interactions.

4. Experimental Section

General Procedures: The optimized structures and single-point energies were calculated by Gaussian03[22] at the B3LYP 6–31G(d) and 6–311+G(d,p) levels, respectively. ^{1}H NMR spectra were recorded on a JEOL 400 (400 MHz) spectrometer. Mass spectra were obtained using a JEOL JMS-K9 mass spectrometer. Differential scanning calorimetry was performed using a Perkin-Elmer Diamond DSC Pyris instrument under nitrogen atmosphere at a heating rate of 10 °C min^{-1}. Thermogravimetric analysis was undertaken using a SEIKO EXSTAR 6000 TG/DTA 6200 unit under nitrogen atmosphere at a heating rate of 10 °C min^{-1}. UV–vis spectra were measured using a Shimadzu UV-3150 UV–vis–near-infrared (NIR) spectrophotometer. Photoluminescence spectra were measured using a FluroMax-2 (Jobin-Yvon-Spex) luminescence spectrometer. The ionization potentials were determined by ultraviolet photoelectron spectroscopy (UPS). The phosphorescent spectra were measured using a streak camera (C4334 from Hamamatsu Photonics) at 4.2 K.

*Synthesis of Tetrachloride (**3**)*: 4,6-Dichloro-2-methylpyrimidine (**1**) (3.14 g, 19.2 mmol) and 3,5-dichlorophenyl boronic acid (8.08 g, 42.3 mmol) were added to a round bottom flask. Acetonitrile (300 mL) and aqueous Na_2CO_3 (1 M, 100 mL) were added and nitrogen bubbled through the mixture for 1 hour. Then, $PdCl_2(PPh_3)_2$ (0.67 g, 0.60 mmol) was added and the resultant mixture was stirred for 6 hours at 60 °C under N_2 flow. The precipitate was filtered, and washed with water and methanol. The resulting off-white solid was dissolved in reflux toluene 450 mL, filtered through a silica-gel pad (50 cc) and washed with toluene (50 mL). After the clear filtrate was concentrated to 50 mL, the precipitate was collected, washed with hexane, dried in vacuo to afford **3** (7.4 g, 81%) as a white solid: ^{1}H NMR (400 MHz, $CDCl_3$) δ = 8.02 (d, 4H, J = 2.0 Hz), 7.77 (s, 1H), 7.51 (t, 2H, J = 2.0 Hz), 2.86 (s, 3H) ppm; MS: m/z 384 $[M]^+$.

Synthesis of B3PyMPM: 3-(4,4,5,5-Tetramethyl-1,3,2-dioxaborolan-2-yl)pyridine (**4**) (4.7 g, 22.9 mmol) and **3** (2.0 g, 5.2 mmol) were added to a round bottom flask. 1,4-Dioxane (220 mL) and aqueous K_3PO_4 (1.35 M, 60 mL) were added and nitrogen bubbled through the mixture for 1 hour. Then, $Pd_2(dba)_3$ (0.19 g, 0.21 mmol) and PCy_3 (0.14 g, 0.50 mmol) were added and the resultant mixture was vigorously stirred for 30 hours at reflux temperature under N_2 flow. The precipitate was filtered, and washed with water and methanol. The resulting off-white solid was purified by chromatography on silica gel (eluent: $CHCl_3/CH_3OH$ = 50:1 to 30:1 v/v) to afford B3PyMPM (2.9 g, 77%) as a white solid: ^{1}H NMR (400 MHz, $CDCl_3$): δ = 8.99 (d, 4H, J = 2.8 Hz), 8.68–8.67 (m, 4H), 8.37–8.36 (m, 4H), 8.06 (s, 1H), 8.03–8.02 (m, 4H), 7.91 (s, 2H), 7.45 (dd, 4H, J = 4.8, 8.0 Hz), 2.94 (s, 3H) ppm; MS: m/z 555 $[M]^+$; Anal. Calcd for $C_{37}H_{26}N_6$: C, 80.12; H, 4.72; N, 15.15%. Found: C, 80.22; H, 4.69; N, 15.22%.

Synthesis of B4PyMPM: B4PyMPM was synthesized by the same procedure using 4-(4,4,5,5-Tetramethyl-1,3,2-dioxaborolan-2-yl)pyridine (**5**) instead of **4**. For B4PyMPM: ^{1}H NMR (400 MHz, $CDCl_3$): δ = 8.77–8.75 (m, 8H), 8.44 (d, 4H, J = 2.0 Hz), 8.04 (s, 1H), 8.00 (t, 2H, J = 1.6 Hz), 7.66–7.64 (m, 8H), 2.95 (s, 3H) ppm; MS: m/z 555 $[M]^+$; Anal. Calcd for $C_{37}H_{26}N_6$: C, 80.12; H, 4.72; N, 15.15%. Found: C, 80.28; H, 4.66; N, 15.20%.

*Synthesis of Tetraboronate Ester (**7**)*: Bis(pinacolato)diboron (**6**) (19.8 g, 78.1 mmol), **3** (6.00 g, 15.6 mmol) and KOAc (18.4 g, 187.2 mmol) were added to a round bottom flask. Anhydrous 1,4-dioxane (300 mL) were added and nitrogen bubbled through the mixture for 1 hour. Then, $Pd_2(dba)_3$ (1.70 g, 1.87 mmol) and PCy_3 (2.50 g, 8.98 mmol) were added and the resultant mixture was vigorously stirred for 18 hours at reflux temperature under N_2 flow. The resulting mixture was cooled to room temperature, and the precipitate was filtered off. To the resulting solution, 300 mL chloroform was added, washed with water and brine, dried over anhydrous $MgSO_4$, filtered, and evaporated to dryness. The resulting solid was purified by chromatography on silica gel (eluent: $CHCl_3$/EtOAc = 3:1 v/v) to afford **7** (7.1 g, 61%) as a white solid: ^{1}H NMR (400 MHz, $CDCl_3$) δ = 8.59 (s, 4H), 8.40 (s, 2H), 7.99 (s, 1H), 2.88 (s, 3H), 1.37 (s, 48H) ppm; MS: m/z 751 $[M]^+$.

Synthesis of B2PyMPM: 2-Bromopyridine (**8**) (5.3 g, 33.3 mmol) and **7** (5.0 g, 6.7 mmol) were added to a round bottom flask. Toluene (200 mL), ethanol (100 mL) and aqueous Na_2CO_3 (1.0 M, 80 mL) were added and nitrogen bubbled through the mixture for 1 hour. Then, $Pd(PPh_3)_4$ (1.54 g, 1.33 mmol) was added and the resultant mixture was vigorously stirred for 12 hours at reflux temperature under N_2 flow. The resulting mixture was cooled to room temperature, washed with water, dried over anhydrous $MgSO_4$, filtered, and evaporated to dryness. The resulting yellow solid was purified by chromatography on silica gel (eluent: $CHCl_3$) to afford B2PyMPM (3.1 g, 84%) as a white solid: ^{1}H NMR (400 MHz, $CDCl_3$): δ = 8.86 (d, 4H, J = 1.4 Hz), 8.80 (t, 2H, J = 1.4 Hz), 8.76 (d, 4H, J = 4.6 Hz), 8.28 (s, 1H), 7.99 (d, 4H, J = 8.2 Hz), 7.83 (ddd, 4H, J = 8.2, 8.2, 2.0 Hz), 7.30 (dd, 4H, J = 4.6, 8.2 Hz), 2.95 (s, 3H) ppm; MS: m/z 555 $[M]^+$; Anal. Calcd for $C_{37}H_{26}N_6$: C, 80.12; H, 4.72; N, 15.15%. Found: C, 80.14; H, 4.54; N, 15.17%.

Supporting Information

Supporting Information is available from the Wiley Online Library or from the author.

Acknowledgements

We greatly acknowledge the financial support in part by the New Energy and Industrial Technology Development Organization (NEDO) through the

"Advanced Organic Device Project" and by the Japan Regional Innovation Strategy Program by the Excellence (J-RISE) (creating international research hub for advanced organic electronics) of the Japan Science and Technology Agency (JST).

Received: June 19, 2010
Published online: October 19, 2010

[1] a) J. Kido, M. Kimura, K. Nagai, *Science* **1995**, *267*, 1332; b) B. W. D'Andrade, S. R. Forrest, *Adv. Mater.* **2004**, *16*, 1585; c) Y. Sun, N. C. Giebink, H. Kanno, B. Ma, M. E. Thompson, S. R. Forrest, *Nature* **2006**, *440*, 908; d) F. So, J. Kido, P. Burrows, *MRS Bull.* **2008**, *33*, 663; e) S. Reineke, F. Lindner, G. Schwartz, N. Seidler, K. Walzer, B. Lüssem, K. Leo, *Nature* **2009**, *459*, 234; f) G. Schwartz, S. Reineke, T. C. Rosenow, K. Walzer, K. Leo, *Adv. Funct. Mater.* **2009**, *19*, 1319.

[2] H. Yersin, Ed. *Highly Efficient OLEDs with Phosphorescent Materials*, Wiley-VCH, Weinheim, **2008**.

[3] a) M. A. Baldo, S. L. Lamansky, P. E. Burrows, M. E. Thompson, S. R. Forrest, *Appl. Phys. Lett.* **1999**, *75*, 4; b) Y. Kawamura, K. Goushi, J. Brooks, J. J. Brown, H. Sasabe, C. Adachi, *Appl. Phys. Lett.* **2005**, *86*, 071104.

[4] a) H. Sasabe, E. Gonmori, T. Chiba, Y.-J. Li, D. Tanaka, S.-J. Su, T. Takeda, Y.-J. Pu, K. Nakayama, J. Kido, *Chem. Mater.* **2008**, *20*, 5951; b) S.-J. Su, H. Sasabe, T. Takeda, J. Kido, *Chem. Mater.* **2008**, *20*, 1691; c) H. Sasabe, Y.-J. Pu, K. Nakayama, J. Kido, *Chem. Commun.* **2009**, 6655.

[5] a) D. Tanaka, H. Sasabe, Y.-J. Li, S.-J. Su, T. Takeda, J. Kido, *Jpn. J. Appl. Phys.* **2007**, *46*, L10; b) H. Sasabe, T. Chiba, S.-J. Su, Y.-J. Pu, K. Nakayama, J. Kido, *Chem. Commun.* **2008**, 5821; c) Y.-J. Li, H. Sasabe, S.-J. Su, D. Tanaka, T. Takeda, Y.-J. Pu, J. Kido, *Chem. Lett.* **2010**, *39*, in press.

[6] S.-J. Su, E. Gonmori, H. Sasabe, J. Kido, *Adv. Mater.* **2008**, *20*, 4189.

[7] a) A. P. Kulkarni, C. J. Tonzola, A. Babel, S. A. Jenekhe, *Chem. Mater.* **2004**, *16*, 4556; b) G. Hughes, M. R. Bryce, *J. Mater. Chem.* **2005**, *15*, 94.

[8] a) S.-J. Su, Y. Takahashi, T. Chiba, T. Takeda, J. Kido, *Adv. Funct. Mater.* **2009**, *19*, 1260; b) S.-J. Su, T. Chiba, T. Takeda, J. Kido, *Adv. Mater.* **2008**, *20*, 2125.

[9] a) H. Bässler, *Phys. Status Solidi B* **1993**, *175*, 15; b) (Eds: P. M. Borsenberger, D. S. Weiss), *Organic Photoreceptors for Imaging Systems*, Marcel Dekker Inc., New York, **1993**.

[10] P. Marsal, I. Avilov, D. A. da Silva Filho, J. L. Brédas, D. Beljonne, *Chem. Phys. Lett.* **2004**, *392*, 521.

[11] N. Schultheiss, E. Bosch, *Heterocycles* **2003**, *60*, 1891.

[12] N. Kudo, M. Perseghini, G. C. Fu, *Angew. Chem. Int. Ed.* **2006**, *45*, 1282.

[13] a) T. Ishiyama, M. Murata, N. Miyaura, *J. Org. Chem.* **1995**, *60*, 7508; b) T. Ishiyama, K. Ishida, N. Miyaura, *Tetrahedron* **2001**, *57*, 9813.

[14] A. Suzuki, H. C. Brown, *Organic Synthesis via Boranes, vol. 3, Suzuki coupling*, Aldrich Chemical Company, Milwaukee, **2003**.

[15] M. A. El-Sayed, *J. Chem. Phys.* **1963**, *38*, 2834.

[16] V. Coropceanu, J. Cornil, D. A. da Silva Filho, Y. Olivier, R. Silbey, J.-L. Brédas, *Chem. Rev.* **2007**, *107*, 926.

[17] a) H.-W. Lin, C.-L. Lin, H.-H. Chang, Y.-T. Lin, C.-C. Wu, Y.-M. Chen, R.-T. Chen, Y.-Y. Chien, K.-T. Wong, *J. Appl. Phys.* **2004**, *95*, 881; b) H.-W. Lin, C.-L. Lin, C.-C. Wu, T.-C. Chao, K.-T. Wong, *Org. Electron.* **2008**, *8*, 189; c) D. Yokoyama, A. Sakaguchi, M. Suzuki, C. Adachi, *Appl. Phys. Lett.* **2008**, *93*, 173302; d) D. Yokoyama, A. Sakaguchi, M. Suzuki, C. Adachi, *Org. Electron.* **2009**, *10*, 127.

[18] L. Bartels, *Nat. Chem.* **2010**, *2*, 87.

[19] a) C. Meier, U. Ziener, K. Landfester, P. Weihrich, *J. Phys. Chem. B* **2005**, *109*, 21015; b) M. Winkler, K. N. Houk, *J. Am. Chem. Soc.* **2007**, *129*, 1805.

[20] a) D. Yokoyama, Y. Setoguchi, A. Sakaguchi, M. Suzuki, C. Adachi, *Adv. Funct. Mater.* **2010**, *20*, 386; b) D. Yokoyama, A. Sekiguchi, M. Suzuki, C. Adachi, *Appl. Phys. Lett.* **2009**, *95*, 243303.

[21] D. Yokoyama, H. Sasabe, Y. Furukawa, C. Adachi, J. Kido, unpublished.

[22] M. J. Frisch et al. Gaussian 03; Gaussian Inc.: Pittsburgh, PA **2003**.